Experimental Study on Statistical Characteristic of MIMO Sensor for Event Detection

Shinji ITABASHI[1], Hiroyoshi YAMADA[2], Kentaro NISHIMORI[3], and Yoshio YAMAGUCHI[4]
[1]Graduate School of Science & Technology, Niigata University
Ikarashi 2-8050, Nishi-ku, Niigata, 950-2181 Japan
[2,3,4]Faculty of Engineering, Niigata University
Ikarashi 2-8050, Nishi-ku, Niigata, 950-2181 Japan

***Abstract*—Recently, researches on radio wave security sensors by using array antenna or MIMO(Multiple-Input Multiple Output) system have been attracting attention. These sensors utilize the property that MIMO channel matrix is sensitive to the propagation environment change in indoor multipath environment. Now the property is used for event detection, such as intrusion, by calculating correlation of MIMO channel matrices. Fundamental study has been performed, however, statistical property, or quantitative detection performance analysis, of the sensor was still remain to be clarified. So, our objective is to derive a probability density function (PDF) of the correlation coefficient and to demonstrate them experimentally. The PDF is a key function to derive detection rate and so on. In the conventional MIMO sensor, correlation coefficient of the channel matrix between with and without an event is used as a measure of events. Therefore, in this report we will derive the PDF of the channel correlation used in the conventional MIMO sensor theoretically and also show the validity by experimental results.**

I. Introduction

Recently, researches on radio wave security sensors by using array antenna or MIMO (Multiple Input Multiple Output) system have been attracting attention. Various systems and detection algorithms have been proposed and examined, and validity of them is shown by simulations and/or experiments to some extent. However, these considerations were done under some specific system and antenna arrangement in a given propagation environment, hence they may often lack in generality. Actually, the quality assessment in consideration of detection probability analysis in given false alarm rate will be required. We found that the channel coherence defined by the MIMO event detection sensor has the same form as that used in the interferometry for Synthetic Aperture Radar image analysis, then we apply the theory to derive theoretical expression of the PDF. The PDF can be evaluated by histogram of the correlation values obtained by experiments. The PDF is the important function to derive detection probability at given false alarm rate theoretically with given event at the SNR. The validity of the derived theoretical expression for channel coherence in MIMO sensor

Therefore, in this report, we show validity of the PDF of the MIMO sensor experimentally by using histograms of the measured MIMO channels

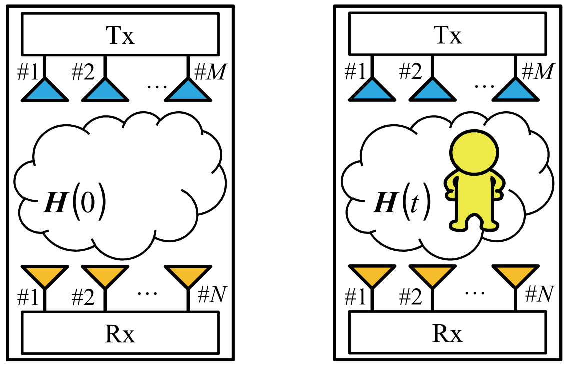

(a) no intrusion (b) intrusion

Fig. 1. MIMO sensor principle figure

II. Indoor invasion detection system

In this chapter, we describe signal model for the MIMO sensor and derive a MIMO channel correlation coefficient.

Figure 1 shows an example of MIMO sensor. In this report, we assume that the sensor is operated in an indoor rich-multipath environment, and also assumes that we employ the MIMO sensor with M transmitting and N receiving antennas. Here, we define the channel matrix without and with the event by $\boldsymbol{H}(0)$ and $\boldsymbol{H}(t)$, respectively as shown in Figs. 1(a) and (b). The MIMO sensor assumed in this report catches change of the propagation channel, and detects the event.

A. Signal model for MIMO sensor

In this report, each transmitting antenna transmits independent signals, then the the received data at time t by the m-th $(= 1, 2, \cdots, M)$ transmitting antenna can be given by

$$\boldsymbol{y}_m(t) \quad = \quad \boldsymbol{h}_m(t) s_m(t) + \boldsymbol{n}_m(t) \tag{1}$$

where $\boldsymbol{h}_m(t)$ is a N dimension propagation channel vector by the m-th transmitting channel, $s_m(t)$ is the transmitting signal (known training symbols), and $\boldsymbol{n}_m(t)$ is the additive Gaussian noise vector having zero mean and power of σ_n^2 in each elements. The MIMO channel matrix can be defined by

$$\boldsymbol{H}(t) \quad = \quad [\boldsymbol{h}_1(t), \cdots, \boldsymbol{h}_M(t)] \tag{2}$$

The MIMO sensor detects the channel change. When we define the channel matrix without the event as $\boldsymbol{H}(0)$ as shown in Fig.1(a), the channel variation, $\boldsymbol{H}_d(t)$, can be defined by

$$\boldsymbol{H}_d(t) \quad = \quad \boldsymbol{H}(0) - \boldsymbol{H}(t) \tag{3}$$

In this report, we assume that the MIMO sensor operates at relative high frequency band (e.g. 2.5 GHz), hence change of the propagation channel by intrusion/event intercepts some paths between transmission and reception. Namely, all the intercepted paths in $\boldsymbol{H}_d(t)$ by the intrusion are independent of the remain paths in $\boldsymbol{H}(t)$ not intercepted by the intrusion. As shown in Fig.1, a propagation channel including propagation information is changed by event sensitively. Therefore, the system which detects propagation information from a received signal is required. The channel vector can be estimated by known training symbol(s). It can be done by [3].

$$\hat{\boldsymbol{h}}_m(t) = \frac{E\left[\boldsymbol{y}_m(t)s_m^*(t)\right]}{E\left[s_m(t)s_m^*(t)\right]} \tag{4}$$

where * is complex conjugate, and $E[\cdot]$ denoted ensemble average.

The MIMO channel correlation can be defined by

$$\rho(t) = \frac{\sum_{n=1}^{N}\sum_{m=1}^{M}\hat{h}_{nm}^*(0)\hat{h}_{nm}(t)}{\sqrt{\sum_{n=1}^{N}\sum_{m=1}^{M}|\hat{h}_{nm}(0)|^2}\sqrt{\sum_{n=1}^{N}\sum_{m=1}^{M}|\hat{h}_{nm}(t)|^2}} \tag{5}$$

where $\hat{h}_{nm}(0)$ and $\hat{h}_{nm}(t)$ are the matrix element at the reference and measured MIMO channel matrix of $\boldsymbol{H}(0)$ and $\boldsymbol{H}(t)$, respectively.

III. Statistical Character of a Correlation Coefficient

Theoretical evaluation of (5) is difficult, however the following formula can be easily calculated.

$$\begin{aligned}\bar{\rho} &= \frac{E\left[\sum_{n=1}^{N}\sum_{m=1}^{M}\hat{h}_{nm}^*(0)\hat{h}_{nm}(t)\right]}{\sqrt{E\left[\sum_{n=1}^{N}\sum_{m=1}^{M}|\hat{h}_{nm}(0)|^2\right]}\sqrt{E\left[\sum_{n=1}^{N}\sum_{m=1}^{M}|\hat{h}_{nm}(t)|^2\right]}} \\ &= \frac{P_0 - P_d}{\sqrt{P_0 + P_E}\sqrt{P_0 - P_d + P_E}}\end{aligned} \tag{6}$$

where P_0 and P_d are the channel power of $\boldsymbol{H}(0)$ and $\boldsymbol{H}_d(t)$, respectively, and P_E is the estimated power of the change components. These power components can be given as follows,

$$P_0 = E\left[\|\ \boldsymbol{H}(0)\ \|_F^2\right], \tag{7}$$

$$P_d = E\left[\|\ \boldsymbol{H}_d(t)\ \|_F^2\right], \tag{8}$$

$$P_E = \frac{M}{N_s}N{\sigma_n}^2, \tag{9}$$

where N_s is snapshot and $||\cdot||_F$ denotes Frobenius norm.

Obviously, the equation (6) is not the correct estimated value for (5). However, this type of correlation is the same form as that in complex coherence in SAR interferometry [2].

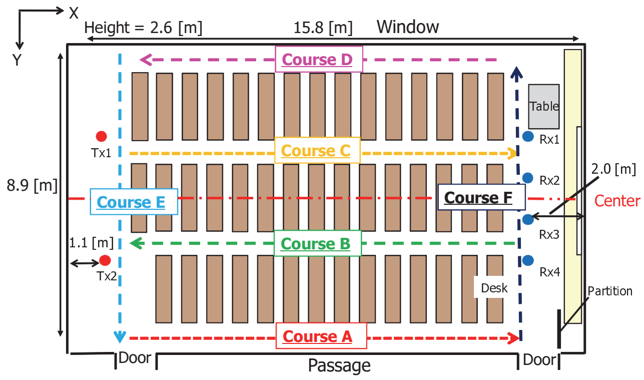

Fig. 2. Measurement environment

TABLE I
Experimental Setup

Tx and Rx antennas ($M \times N$)	2×4
Receiving array shape	Uniform linear array
RF frequency	2.55 [GHz]
Total power	0 [dBm]
Element interval(Rx)	1.2 [m]
Element interval(Tx)	3.6 [m]
Antenna height	1.0 [m]
Training symbol(snaphots)	160 symbols

According to [2], the probability density function (PDF) of (6) can be given by

$$\begin{aligned}f(\rho) = 2(L-1)(1-\bar{\rho}^2)^L\rho(1-\rho^2)^{L-2} \\ \times\ {}_2F_1(L, L; 1; \bar{\rho}^2\rho^2)\end{aligned} \tag{10}$$

where $\Gamma(\cdot)$ and ${}_aF_b$ are the Gamma and generalized hypergeometric function, respectively, and $L = NM$.

IV. Experimental Study

A. Measurement environment

Measurement environment is shown in Fig. 2, and experimental setup is shown in Table I. In this environment, we carried out several experiment with and without a walker. The walking (observation) time at the courses A∼D was 12 seconds each, and the courses E∼F was 8 each.

B. Experimental Results

1) CASE I: No intrusion: The theoretical PDF is calculated at given SNR and ISR values. However, the received power of experimental data were little bit fluctuated, so we used the data in 1 dB power bandwidth at the target value (target value ±0.5 dB). The target value is also estimated by making histogram of power distribution for the measured MIMO channel.

The SNR is received power versus the noise power ratio without event (no intrusion), and the ISR is defined by the changed power with the event (intruder) versus received power

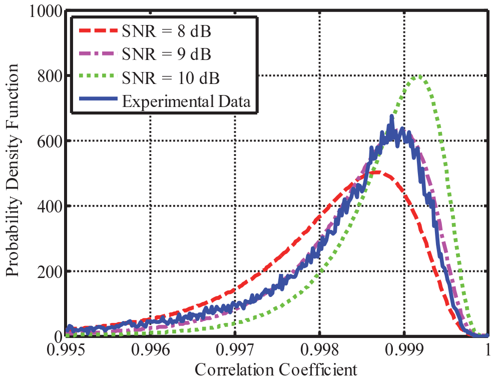

Fig. 3. PDF (w/o intrusion)

without the event. Their definition can be written by

$$\mathrm{SNR} = 10\log_{10}\frac{P_0}{P_N} \quad [\mathrm{dB}] \tag{11}$$

$$\mathrm{ISR} = 10\log_{10}\frac{P_d}{P_0} \quad [\mathrm{dB}] \tag{12}$$

Direct measurement of the noise power for the system used in this experiment was difficult. So, in this experiment, the SNR was experimentally evaluated by the estimated PDF derived by the histogram of MIMO correlation without event. The experimental result and the several theoretical PDFs for SNR=8, 9, and 10 dB, are shown in Fig. 3. From Fig. 3, it turns out that the experimental result is almost coincide with the theoretical PDF of SNR=9 dB. This shows that SNR in the measurement environment in this experiment was 9 dB. Moreover, since the theoretical and the experimental curves agree well, the theoretical PDF in (10) is valid in this indoor MIMO sensor at 2.55 GHz.

2) CASE II: With Intrusion:

Also with intrusion, the same experimental setups as without the intrusion were used. And, in order to check the validity of the theoretical expression for the PDF with intrusion, the histograms are created by the experimental data with each intrusion, and we evaluate the result of each course. Especially, we focus on the results at the course A, B, and F.

In this case with intrusion, direct measurement of P_d is difficult and it may change at some extent with behavior of the walker, then the ISR is also estimated in comparison with theoretical plots of PDF for several different ISRs.

First, the result of the course A is shown in Fig. 4. From this figure, the ISR in this path can be estimated almost -15 dB by the corresponding theoretical curve. The histogram of ISR estimated by the experimental data is also shown in Fig. 5. From Fig. 5, it turns out that peak of ISR in this experiment was -15 dB and it is almost coincide with the estimated value in Fig. 4. In Fig. 4, the experimentally derived PDF looks slightly distorted to the theoretical curve. This is because we evaluate the experimental data including all ISR values in Fig. 5. The number of data is limited in this case, hence we could not evaluate the narrow power-bandwidth ISR data at around -15 dB. However, there results show that the theoretical and experimental distribution is well coincide with each other.

Next, the result of the course B is shown in Fig. 6. From Fig. 6, the estimated ISR in this case becomes -10 dB which was slightly larger change in comparison with that in course A. Likewise in the previous results, the histogram in this experimental data set in Fig. 7 shows the peak at around -10 dB. This coincides the estimated results in Fig. 6.

Finally, we would like to show the results of course F as the differently directed path for course A and B. Result of PDF for this course is shown in Fig. 8.In this case, distortion of the experimental curve is larger than the previous results, and we could hardly estimate the ISR, but the ISR would be in the range between -10 to -15 dB. The cause of distortion can be realized by the histogram shown in Fig. 9. The ISR in this course spreads widely. Obviously, this causes because the course F across the receiving array. The incoming path in each receiving element changes a lot in comparison with the course of along direction.

From these result, we can conclude that the theoretical expression for the PDF is valid with and without the event by the experimental results.

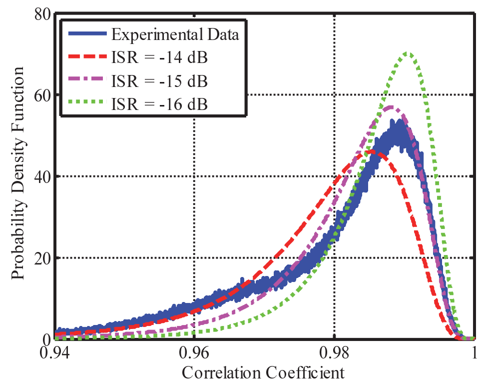

Fig. 4. PDF(w/ intrusion) of Course A

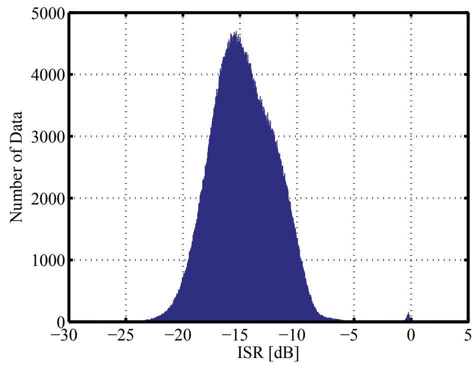

Fig. 5. Histogram of ISR(Course A)

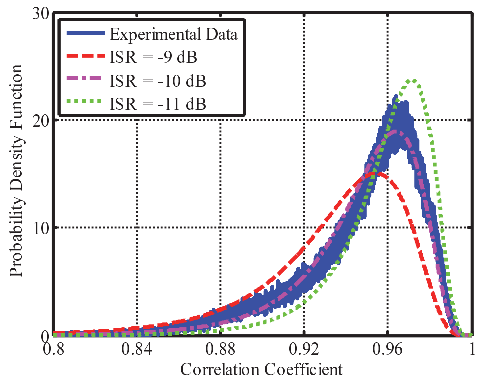

Fig. 6. PDF(w/ intrusion) of Course B

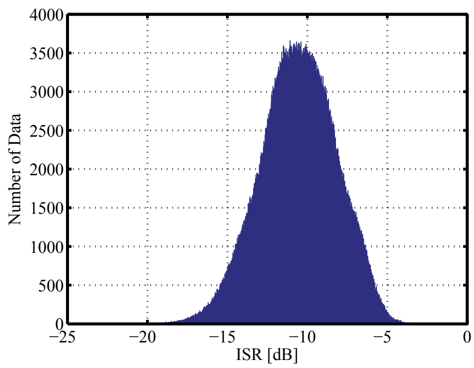

Fig. 7. Histogram of ISR(Course B)

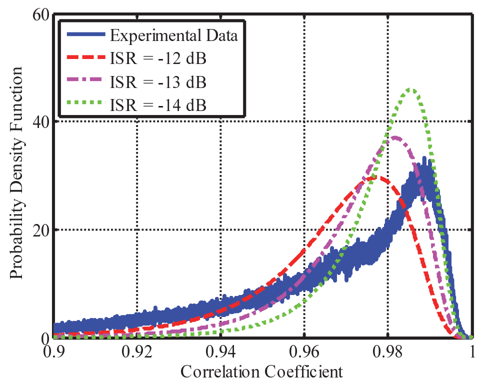

Fig. 8. PDF(w/ intrusion) of Course F

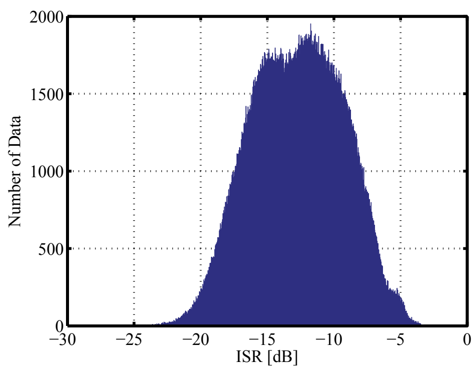

Fig. 9. Histogram of ISR(Course F)

V. Conclusion

In this report, we show the theoretical expression of the MIMO channel correlation by using the results of complex coherence in SAR interferometry. In addition, we show the validity of the theoretical expression by the experimental data set acquired in the actual indoor rich-multipath environment.

In the experiment, the noise power and the changed power by the event could not be measured. However, the estimated values agreed well with the total power distribution and ISRs. These results support for availability of this theory. By using this PDF, the detection probability can be easily estimated. This expression will be available for relative high frequency case. For application of MIMO sensor in low frequency below 1 GHz, some modification will be required. This wiil be the one of future works.

Acknowledgment

This work is supported by JSPS KAKENHI, the Grant-in-Aid for Scientific Research (C) (No.23560442).

References

[1] S.Ikeda, H.Tsuji, T.Ohtsuki, "Indoor Event Detection with Eigenvector Spanning Signal Subspace for Home or Office Security," IEICE Trans. Commun., vol.E-92-B, no.7, pp.2406-2412, July 2009.

[2] R.Touzi, A.Lopes, J.Bruniquel, P.W.Vachon, "Coherence Estimation for SAR Imagery," IEEE Trans. Geosci. Remote Sensing., vol.37, no.1, pp.135-149, Jan. 1999.

[3] M. Biguesh, A. B. Gershman, "Training-Based MIMO Channel Estimation :A Study of Estimator Treadeoffs and Optimal Training Signals" IEEE Trans. Signal Process., vol.54, no.3, pp.884-893, Mar. 2006.